Widom and extrema lines as criteria for optimizing operating conditions in supercritical processes

Adil Mouahid, Pierre Boivin, Suzanne Diaw, Elisabeth Badens

WIDOM AND EXTREMA LINES AS CRITERIA FOR OPTIMIZING OPERATING CONDITIONS IN SUPERCRITICAL PROCESSES

Adil Mouahid, Pierre Boivin, Suzanne Diaw, Elisabeth BADENS*

Aix Marseille Univ, CNRS, Centrale Marseille, M2P2, Marseille, France

*Corresponding author: Elisabeth.badens@univ-amu.fr

Nomenclature

a	interaction parameter ($J{\cdot}m^3{\cdot}mol^{-2}$)
b	co-volume ($m^3{\cdot}mol^{-1}$)
C_p	heat capacity at constant pressure ($J{\cdot}mol^{-1}{\cdot}K^{-1}$)
C_v	heat capacity at constant volume ($J{\cdot}mol^{-1}{\cdot}K^{-1}$)
M	molar mass ($g{\cdot}mol^{-1}$)
R	ideal gas constant ($J{\cdot}mol^{-1}{\cdot}K^{-1}$)
P	pressure (Pa)
T	temperature (K)
v	molar volume ($m^3{\cdot}mol^{-1}$)
x	heavy key molar fraction
Z	compressibility factor

Subscript

1	more volatile compound: CO_2
2	less volatile compound: organic solvent
c	critical
m	mixture
r	reduced

Superscript

Id	ideal
R	reel

Greek letters

ω	acentric factor
ρ	density ($kg{\cdot}m^{-3}$)

1. Introduction

The specific properties of supercritical fluids (SCF) are exploited in a wide range of applications, whose numbers continue to steadily grow. SCF are used today in processes of i) extraction, fractionation, purification or cleaning, ii) formulation, shaping or functionalization of materials, iii) chemical reaction for synthesis or degradation, iv) sterilization [1-5]. Extraction using supercritical carbon dioxide (sc CO_2) is the most commonly studied application in research laboratories and the most developed in the industry. For all the above applications, operating conditions, and in particular pressure and temperature are chosen to achieve high process efficiency while minimizing energy consumption and preventing product degradation. When the process involves a step of solute solubilization in the supercritical phase, the operating conditions are chosen to favor high solute solubility. A higher pressure, corresponding to a higher SCF density, may lead to a higher solubility. The current trend in the industry for the extraction of polar compounds with supercritical carbon dioxide is to increase pressure in order to increase solute solubility in CO_2 and avoid the use of a polar co-solvent or modifier. Regarding the temperature, it is necessary to identify the retrograde solubility zone as it is known that within the retrograde zone, an increase in temperature leads to a decrease in the solute solubility while outside that zone, for higher pressures, an increase in temperature leads to an increase in solubility. The density of the SCF is the key-parameter taken into account for the choice of operating conditions, as well as in the discussion of the results obtained for the majority of SCF applications.

In short, when it comes to delimiting the experimental domain for a given application, a range of pressure and temperature, corresponding to different values of SCF properties is fixed, the area around the critical point being avoided since large fluctuations of these properties are observed for small variations of P and T.

However, additional elements should be integrated into the choice of operating conditions. It is known that two different areas can be distinguished in the supercritical domain: a zone where the fluid has liquid-like properties and one where it has gas-like properties, separated by a boundary line, commonly called the Widom line (see Figure 1(a)). This line was described by Fisher and Widom [6], as the transition zone of the pair-correlation function from an oscillatory (liquid-like) to a monotonous (gas-like) behavior. The pair correlation function is determined from the inverse Fourier transform of the structure factor. The latter can be assessed either by experimental measurements such as neutron scattering or by simulation, for example using the Monte-Carlo method.

Several concepts have been developed to characterize the Widom line. In simple and general terms, this line can be considered as an extension of the liquid-vapor equilibrium line above the critical point. It is a frontier zone in which a phase transition occurs similarly to the liquid-vapor transition observed in the subcritical region. However, below the critical point, the transition takes place at saturation temperature, while in the supercritical region, the transition happens over a finite temperature interval. Thus, the Widom line can also be considered as a pseudo-boiling line (see Figure 1 (b)) [7]. A key point is that this line is the locus of anomalous behaviors or discontinuous changes in fluid properties (compressibility, heat capacities, density, thermal expansivity, speed of sound, …). Therefore, this frontier zone can be located plotting either the extension of the LVE line above the critical point, or the extrema lines for properties such as heat capacity. Lastly, for properties like density or enthalpy, since the property changes for an increase in temperature in this particular region are respectively a dramatic decrease or increase, the inflexion points of each isobaric curves are considered, and an inflexion point line can be thus drawn.

For decades, the concept of this Widom line was confidential, mainly addressed in the context of rocket engines. Several works have nevertheless demonstrated its existence, its

characterization and have brought significant inputs about the equations for its drawing [7-11] for pure compounds as well as for binary mixtures [12].

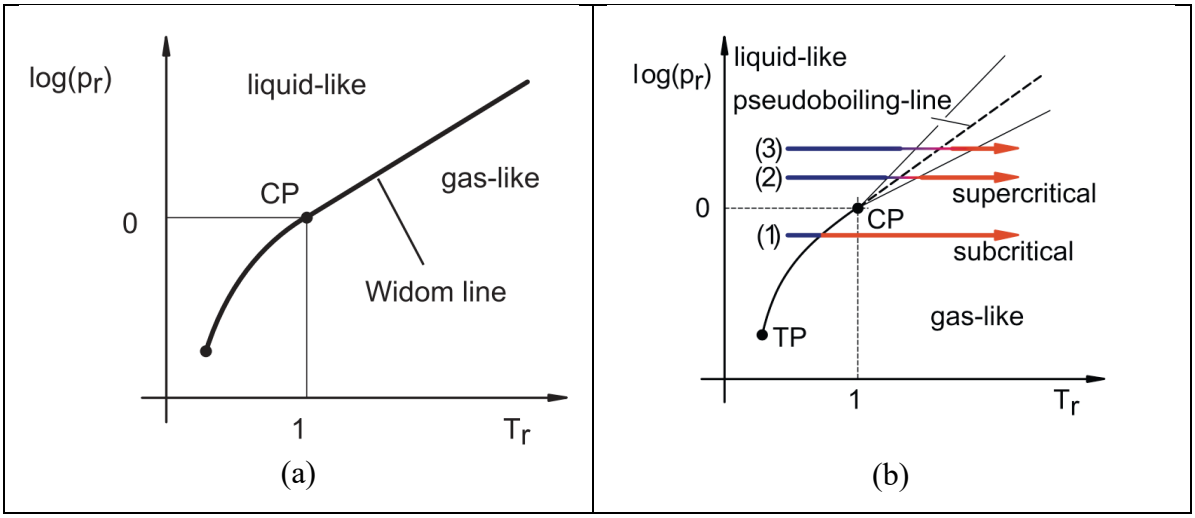

Figure 1 (a): Representation of the Widom line delimiting the two different zones in the supercritical domain, where CP is the critical point, $T_r=T/T_c$ and $P_r=P/P_c$; (b) Representation of the transition zones. (1): transition occurring in the subcritical domain, (2) and (3) transition occurring in the supercritical domain. Figures taken from [7].

The consideration of the Widom line for pure compounds is meaningful only for pressures and temperatures just above the critical coordinates while for higher pressures and temperatures, the fluctuations of the different properties are rapidly mitigated. For illustrative purpose, the variation of the isobaric heat capacity of carbon dioxide as a function of temperature is reported under 80 bar and 100 bar in Figure 2. It can be seen that under 80 bar, just above critical pressure, there are significant fluctuations of the heat capacity over a small range of temperature while under 100 bar, the fluctuations are far weaker.

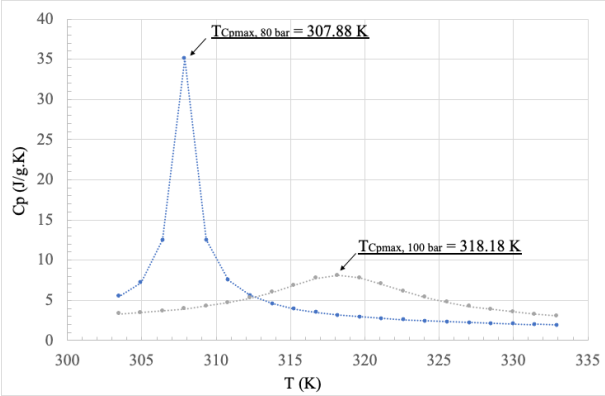

Figure 2 : Isobaric evolution of carbon dioxide heat capacity as a function of temperature (at 80 bar and 100 bar).

Recently, De Jesus *et al.* [13] have estimated the coordinates of the Widom line end points of 5 compounds including carbon dioxide and water. The Widom line end points are represented for carbon dioxide and water respectively in Figure 3 (a) and (b). These end point coordinates are estimated using a quantitative criterion which involves the difference between the temperature maxima of isothermal compressibility ($T_{\beta\ max}$) and the temperature maxima of isobaric heat capacity ($T_{Cp\ max}$): $\Delta T = T_{\beta\ max} - T_{Cp\ max}$. Moving along the Widom line of carbon dioxide, the end point locus corresponds to $\Delta T = 0.001 T_c$ according to Zeron *et al.* [14] or to $\Delta T = 0.005 T_c$ according to De Jesus *et al.* [13], where T_c is the critical temperature of the compound. For carbon dioxide, using the former formula, the coordinates of the end point are (T_{end}=309.65 K; P_{end}=82.29 bar) and using the latter, the coordinates of the end point are (T_{end}=313.91 K; P_{end}=88.56 bar). Similarly, using the same criteria for water, the coordinates of the Widom line end point are respectively (T_{end}=669.74 K; P_{end}=281.32 bar) and (T_{end}=682.68 K; P_{end}=310.66 bar).

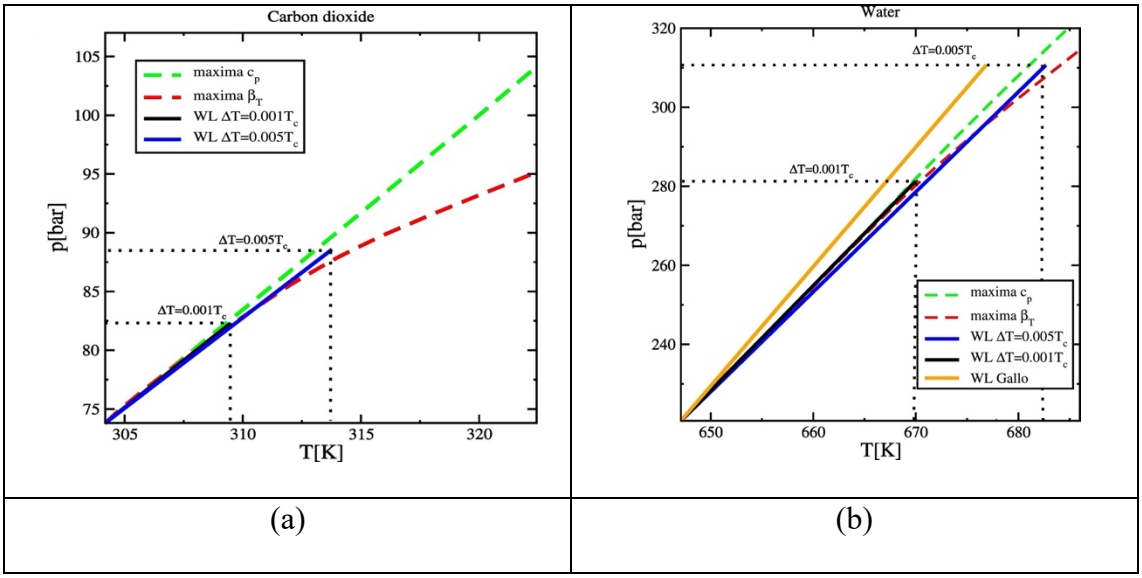

Figure 3 (a) Representation of the carbon dioxide Widom line end point using two different criteria; (b) Representation of the water Widom line end point using two different criteria. Figures taken from [13].

Another approach for the delimitation of the two zones between gas-like and liquid-like behaviors, which uses excess entropy, has been proposed recently by Bell *et al.* [15]. These authors have shown that excess entropy is linked to macroscopically scaled transport properties, related to local structure. They have considered the macroscopic scaled viscosity of some atomic fluids and have highlighted that their minima are observed in a narrow range of excess entropy. For atomic fluids as well as for polyatomic fluids, excess entropy can be evaluated using an equation of state or from molecular dynamics simulation and can be therefore used to demarcate gas-like and liquid-like behaviors in the supercritical region.

As mentioned above, Raju *et al.* [12] studied the Widom lines in binary mixtures. From molecular dynamics simulations, they demonstrate the existence of a single set of Widom lines or of multiple Widom lines depending on the mixture phase behavior type. Binary diagrams of liquid-fluid systems are of 6 types in the classification of Van Konynenburg and Scott [16]. The differences between the different types mainly come from the differences in liquid behavior below the lower of the two critical temperatures; the SCF-fluid behavior may also differ from one type to another.

Figure 4 presents a type I phase diagram projected on a P-T plane. The curves lg are the vapor pressure curves of the pure components which end in a critical point. For type I diagrams, there is only one critical curve and this curve (the dashed line in Figure 4 (a)) runs continuously from the critical point of component A to the critical point of component B. Type I diagrams concern components with quite similar sizes, interaction forces, equivalent molecular diameters or critical coordinates. However, as a general rule, the molar mass and critical temperature of the less volatile components are higher than those of the more volatile components. Figure 4 (b) shows the schematic phase diagram for a non-ideal liquid mixture of type I at a temperature above the critical temperature of the more volatile component. Type III mixtures are characterized by a region of liquid-liquid immiscibility extending to the gas-liquid critical line, thus discontinuous.

Raju *et al.* [12] have studied, among others, the following mixtures of noble gases: Type I (Argon/Krypton) and Type III (Neon/Krypton) binary mixtures. They show that depending on the mixture phase behavior type, the transition from a liquid-like to a gas-like region may be different, following different pathways. They show that miscible binary mixtures of type I have behavior analogous to pure fluid, corresponding to a single liquid-gas transition in the supercritical domain while non-miscible binary mixtures of Type III led to multiple distinct Widom lines. They also highlight that significant changes in fluid properties of binary mixtures are observed for pressures up to 3 P_c of the more volatile compound.

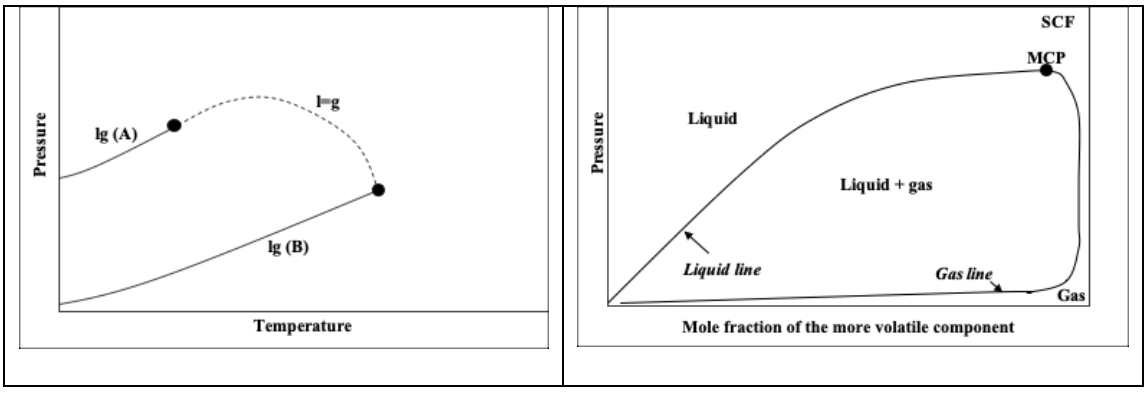

(a)	(b)

Figure 4 (a) Type I phase diagram projected on a P-T plane; (b) Schematic phase diagram for a non-ideal liquid mixture of type I at constant temperature (above the critical temperature of the more volatile component). MCP: Mixture Critical Point.

If we focus on supercritical carbon dioxide, which is the most frequently used SCF, it appears that the Widom line crosses operating domains that are commonly explored. The extrema line of the carbon dioxide heat capacity is plotted in Figure 5 with a focus on the zone just above the critical coordinates. For example, under a pressure of 80 bar, when the temperature ranged from 305 to 318 K, the extrema line of the heat capacity as well as the Widom line are crossed. If an experiment is conducted under 80 bar and 308 K, or under 90 bar and 313 K, the fluid properties may undergo significant fluctuations. Accordingly, whatever the studied application, it would be then recommended to take into account the Widom line and the extrema lines in delimiting the experimental domain as well as to achieve a better interpretation of the results.

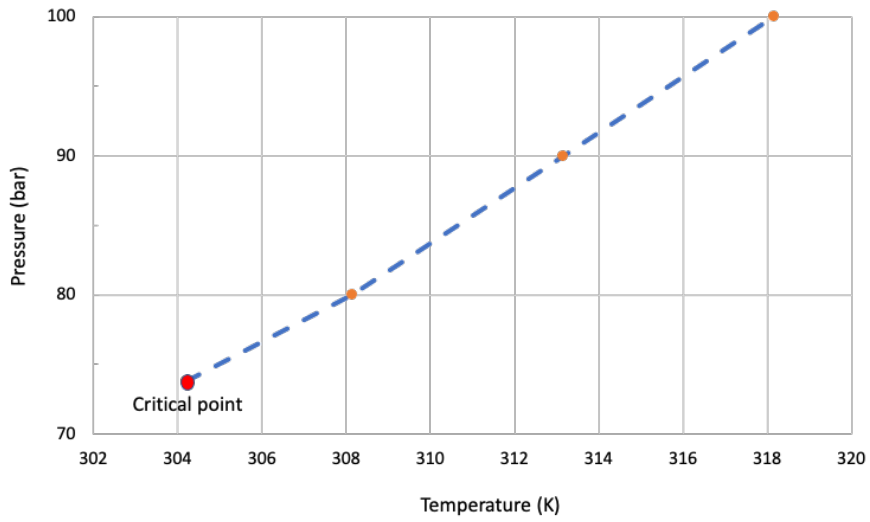

Figure 5 Representation of the extrema line of carbon dioxide heat capacity just above the critical point (data taken from NIST).

Regarding binary mixtures involving sc CO_2, Type I diagrams are often encountered since binary (CO_2 / usual organic solvent) systems are mostly of Type I. This suggests that a single set of Widom lines may exist for binary mixtures involving sc CO_2.

The objective of this work is to plot Widom lines, extrema lines and inflexion point lines for CO_2, eight organic solvents and water, for the pure compounds as well as for binary mixtures involving CO_2. The studied binary mixtures correspond to Type I or Type III phase diagram systems all involving CO_2. The Type I diagrams are observed for binary mixtures involving CO_2 and a light organic solvent: Acetone [17, 18], Acetonitrile [18], Dimethyl Formamide [19], Ethanol [17, 20], Methanol, Methylene Chloride [17, 18], N-Methyl Pyrolidone [18], Tetrahydrofuran [18, 21]. The binary CO_2-water mixture exhibits a Type III diagram [20, 22]. These systems are of interest for a large spectrum of SCF applications, like extraction, cleaning, crystallization, or material processing, when an organic solvent or water are used for modifying the properties of sc CO_2, mainly the polarity. The global compositions of the binary mixtures studied correspond to those commonly used in the aforementioned applications. Mixtures containing 1, 5 and 10 % of organic solvent have been considered. This study brings new data that can be beneficial in the choice and optimization of the operating conditions for supercritical processes.

2. Material and methods

2.1 The selected solvents

Eight organic solvents as well as water were selected for this study as they are involved in different fields of applications. The list of the studied compounds with their critical properties is given in Table 1. The fluid properties were taken from Perry's chemical handbook [23] or from the NIST online database [24]. All the critical coordinates were taken from Perry's. If the

acentric factor ω was not accessible, it was calculated according to Eq. 1 [25]. For the CO_2-solvent binary mixtures, three compositions were considered: $x_1 = 0.5$, $x_1 = 0.9$ and $x_1 = 0.95$.

$$\omega = \frac{3}{7}\left(\frac{{}^{T_b}/_{T_c}}{1-{}^{T_b}/_{T_c}}\right)\log(P_c(atm)) - 1 \qquad (1)$$

Table 1 Critical properties and acentric factor of the selected solvents

Solvent	**M** (g/mol)	$\mathbf{T_c}$ (K)	$\mathbf{P_c}$ (bar)	$\mathbf{V_c}$ ($m^{3.}$ $kmol^{-1}$)	**ω**	**Ref.**
CO_2	44.010	304.21	73.9	0.095	0.224	[23]
Methylene chloride	84.930	508	63.55	0.193	0.240	[24]
Acetone	58.080	508.2	47.1	0.21	0.307	[23]
Methanol	32.042	512.64	81.4	0.117	0.566	[23]
Ethanol	46.0690	513.92	61.2	0.168	0.643	[23]
Tetrahydrofuran (THF)	72.1057	540.2	51.9	0.225	0.238	[24]
Acetonitrile	41.0530	545.5	48.5	0.173	0.340	[23]
Water	18.0150	647.13	219.4	0.056	0.343	[23]
N,N-Dimethyl Formamide (DMF)	73.0950	649.6	43.7	0.262	0.312	[23]
1-methyl-2-pyrrolidone (NMP)	99.1311	721.7	45.2	0.31	0.367	[24]

2.2 Methodology used for the location of the Widom lines, extrema lines and inflexion point lines

On referring to the literature, for single-phase fluids, the location of the Widom line can be calculated? by applying the equations of Banuti [26] and for binary mixtures, molecular dynamics (MD) simulations [12, 27] give convincing results. Indeed, MD simulations lead to accurate calculations as they enable the characterization of microscopic interactions and structures and go further in the fluid behavior knowledge. This tool is increasingly used by researchers, nevertheless, it is a very specific tool that requires particular hands-on skills to be applied.

In this study, another method is adopted for the determination of the Widom lines of CO_2-solvent binary mixtures in the form of a chemical engineering approach, simpler and more straight-forward. Three methods based either on the equations of Banuti or a cubic equation of

states are proposed. The Widom lines were plotted reporting pressure as a function of the temperature for easier exploitation.

2.2.1 Location of the Widom lines using the equations of Banuti [26]

The first calculation method consists of applying the equations of Banuti [26], given in Eq. 2 and 3, for a single-component fluid phase. The binary mixture was then considered as a single-component fluid phase with its specific critical coordinates and acentric factor. The mixture properties were calculated using the methods of Reid and Prausnitz [25] given in Eqs 4 to 9. The Widom line was plotted by selecting a range of temperatures to calculate the equilibrium pressure (Eq. 2).

$$P_r = exp\left[\frac{A_s}{\min(T_r,1)}(T_r,1)\right] \quad (2)$$

$$A_s = 5.51934 + 4.80640\omega - 0.537437\omega^2 \quad (3)$$

$$v_{cm} = \sum x_i x_j v_{cij} \quad (4)$$

$$v_{cij} = \sum[(v_{ci}^{\frac{1}{3}} + v_{cj}^{\frac{1}{3}})^3]/8 \quad (5)$$

$$T_{cm} = \sum x_i x_j T_{cij}(\frac{v_{cij}}{v_{cm}}) \quad (6)$$

$$\omega_m = \sum x_i \omega_i \quad (7)$$

$$Z_{cm} = 0.2905 - 0.085\ \omega_m \quad (8)$$

$$P_{cm} = Z_{cm}(\frac{R.T_{cm}}{v_{cm}}) \quad (9)$$

The calculated properties for the binary mixtures are given as supplementary material.

2.2.2 Location of the heat capacity extrema lines and of the density inflexion point lines using PR EOS

2.2.2a Calculations using classical mixture rules

The second method consisted in applying a cubic equation of state with the classical mixture rules to plot the variations of the mixture density ρ and the mixture isobaric heat capacity C_p over a selected range of pressure and temperature. The C_p extrema lines and the ρ inflexion point lines were then plotted by considering respectively for each pressure, the temperature at the maxima of heat capacity and at the density inflexion point. In general, the calculations were performed for temperature ranges from 313 to 700 K and pressure ranges from 60 to 200 bar.

It was chosen to apply the Peng-Robinson (PR) equation of state (EoS) given in Eqs. 10 to 17

$$P = \frac{RT}{v-b} - \frac{a}{v^2+ubv+wb^2} \quad (10)$$

With:

$$a = a_c f\left(\frac{T}{T_c}\right) \quad (11)$$

$$a_c = \frac{\Omega_a R^2 T_c^2}{P_c} \quad (12)$$

$$f\left(\frac{T}{T_c}\right) = \left(1 + m\left(1 - \sqrt{\frac{T}{T_c}}\right)\right)^2 \quad (13)$$

$$m = m_0 + m_1\omega + m_2\omega^2 \quad (14)$$

$$b = \frac{\Omega_b R T_c}{P_c} \quad (15)$$

For a mixture (i,j):

$$b = \sum x_i b_i \quad (16)$$

$$a = \sum\sum x_i x_j \sqrt{a_i}\sqrt{a_j}\left(1 - k_{ij}\right) \quad (17)$$

$u = 2$, $w = -1$, $\Omega_a = 0{,}4572$, $\Omega_b = 0{,}0778$, $m_0 = 0{,}3746$, $m_1 = 1{,}5423$, $m_2 = -0{,}2699$, k_{ij} was systematically set to 0 for the sake of simplicity.

Calculations were performed by considering the PR EoS in its polynomial form (Eqs. 18 to 24). The calculation method consists in solving Eq. 18 and choosing the solution leading to the calculation of the compressibility factor *Z* (Eq. 19) corresponding to the physical state of the fluid. In the presented case, the solution corresponding to the liquid state (lower real value of *Z*) was chosen for the calculation of the properties. The calculation of density mixture was performed by applying Eq. 25. The temperature at the inflexion point was then determined by plotting the mixture density at a selected pressure for a temperature ranging from 313 to 700 K. The calculations were then performed for another selected pressure. The density inflexion point line was then plotted.

$$Z^3 + C_2 Z^2 + C_1 Z + C_0 = 0 \quad (18)$$

With:

$$Z = \frac{Pv}{RT} \quad (19)$$

$$A = \frac{aP}{(RT)^2} \quad (20)$$

$$B = \frac{bP}{RT} \quad (21)$$

$$C_2 = B - 1 \quad (22)$$

$$C_1 = -3B^2 - 2B + 1 \quad (23)$$

$$C_0 = B^3 + B^2 - A.B \quad (24)$$

$$\rho(kg/m^3) = \frac{P(x_1 M_1 + x_2 M_2)}{Z.R.T} 10^{-3} \quad (25)$$

The heat capacity C_p can be calculated considering Eq. 26 to 29. Nevertheless, for the sake of simplicity, it is sufficient to determine the maxima of C_p^R. The expressions of all derivatives involved for these calculations were given by Pratt [8], for brevity the expression will not be given in this study. The maxima of C_p^R were then determined applying the same method as that described for the density inflexion point.

$$C_p = C_p^{Id} + C_p^R \quad (26)$$

With:

$$C_p^R = C_v^R + T\left(\frac{\partial P}{\partial T}\right)_v \left(\frac{\partial v}{\partial T}\right)_P - R \quad (27)$$

$$C_p^{Id} = x_1 C_{p1}^{Id} + x_2 C_{p2}^{Id} \quad (28)$$

$$C_v^R = \frac{T\frac{d^2a}{dT^2}}{b\sqrt{8}} \ln\left(\frac{Z+B\left(1+\sqrt{2}\right)}{Z+B\left(1-\sqrt{2}\right)}\right) \quad (29)$$

2.2.2b Calculations equating the binary mixture as a single component phase

Similarly to the calculation of the Widom line using the equations of Banuti (§ 2.2.1), the binary mixture is considered as a single-component fluid phase with its critical coordinates and acentric factor calculated thanks to Eqs. 4 to 9. The PR EoS was then applied to calculate the isobaric heat capacity and density as a function of temperature using the same methodology as the one described above (§2.2.2a). The aim of this method was to avoid mixing rules for easier calculations.

3. Results and discussions

3.1 Validation of the proposed methodology

It was chosen to perform the calculations on the equimolar binary mixtures Ar/Kr (type I phase behavior) and Ne/Kr (type III phase behavior) studied by Raju *et al.* [12] to validate our methodology. The three methods described above (§2.2.1, §2.2.2a and §2.2.2b) were applied to predict the binary mixture Widom lines. The methods described in §2.2.2 were also used to determine the binary mixture densities according to temperature. The Widom lines and the binary mixture density variations with temperature were compared with those published by Raju *et al*. [12]. The results are reported in Figure 6.

In Figure 6 (a), the variation of the equimolar Ar/Kr mixture density as a function of temperature is reported at 65 bar and 140 bar. It can be seen on one hand, that the calculation of density considering either a binary mixture or a single-component phase led exactly to the same values of densities for all conditions of pressure and temperature. The same is true for binary mixture

C_p^R calculations. On the other hand, the average relative deviations between the density calculations obtained in this study and the results reported by Raju *et al.* [12] range from 2.95 to 3.02 % for the binary mixture Ar/Kr and from 4.6 to 14.9 % for the binary mixture Ne/Kr. Furthermore, the Widom lines and extrema lines reported in Figure 6 (b) and (d) were congruent with the results published by Raju *et al.* [12] and the results obtained by the three methods proposed in this work. Indeed, the deviations ranged from 0.04 to 5.12 % for Ar/Kr equimolar binary mixture and from 0.63 to 6.2 % for Ne/Kr equimolar binary mixture.

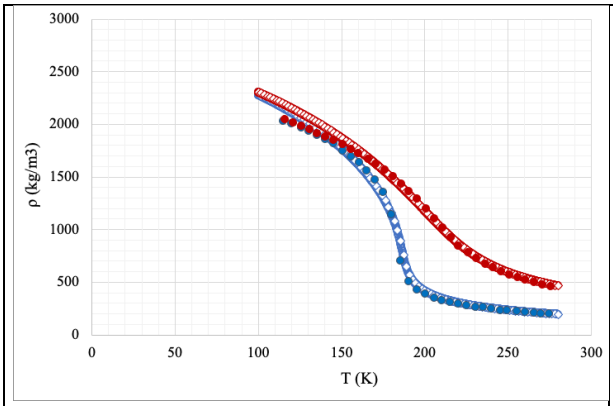

(a)

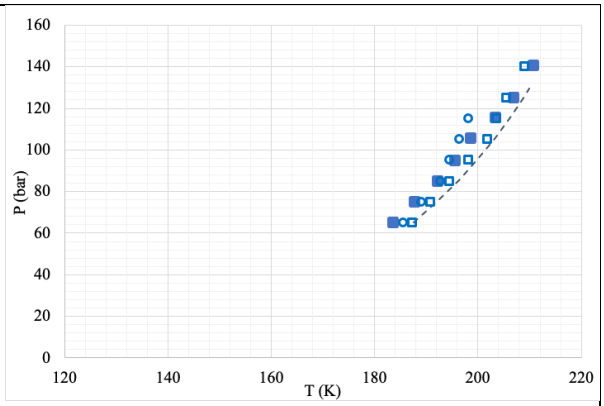

(b)

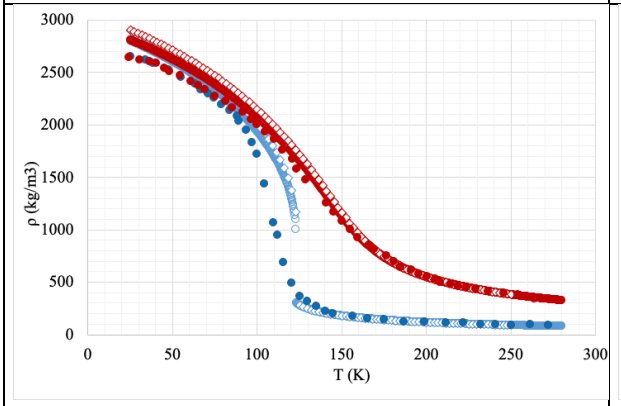

(c)

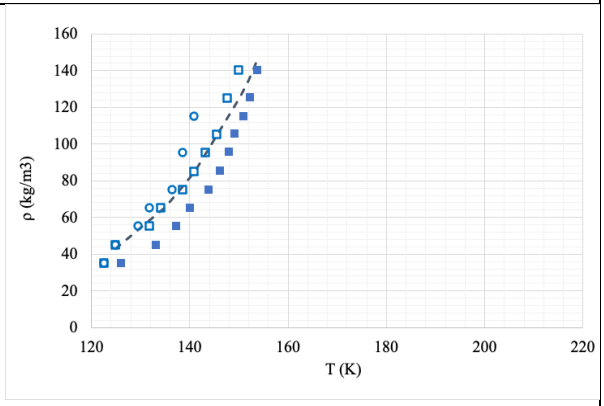

(d)

Figure 6 (a) et (c): Respectively Ar/Kr and Ne/Kr density equimolar mixture variations as a function of temperature, ○ This work – binary mixture 65 bar; ◇ This work – pseudo-single-component 65 bar; ● Raju – 65 bar ; ○ This work – binary mixture 140 bar; ◇ This work – pseudo-single-component 140 bar; ● Raju – 140 bar.
(b) and (d): Widom lines and extrema lines of respectively Ar/Kr and Ne/Kr equimolar mixtures, ■ Raju - Extrema line C_p; □ This work - Extrema line C_p; ○This work – Density inflexion point line; Blue dashed line: This work - Widom line.

In light of these results, it can be concluded that the three proposed methods are well suited in determining the Widom lines on binary mixtures of Type I and type III phase behaviors.

3.2 Widom line, extrema lines and inflexion point lines of pure compounds and of binary mixtures

3.2.1. Type I phase behavior mixtures

The predicted Widom lines, extrema lines and inflexion point lines for pure compounds and for binary mixtures involving CO_2 with the different studied organic solvents are presented in Figures 7 to 14. On each figure, the Widom line of pure CO_2, of pure organic solvent as well as those of the binary mixtures (5, 10 and 50 % of organic solvent) are plotted. The mixture extrema lines and the density inflexion point lines are also plotted. For the sake of clarity, we did not plot the results for other binary mixture compositions. Nevertheless, all the details are given in the previous section for the calculations of any composition.

For each binary mixture, as expected, the different binary mixture lines are close to the Widom line of pure CO_2 for the lowest percentages of organic solvent (5 and 10%). This is less marked for the binary mixtures with DMF or NMP since they have the highest critical temperatures (respectively 649.6 K and 721.7 K). These percentages are often used for extraction, fractionation, cleaning, particle generation as well as for impregnation/functionalization. The results presented here can be useful for all these applications when it comes to the choice of operating conditions. Indeed, the conditions of pressure and temperature must be chosen so as to avoid the pseudo-boiling zone just above the critical point. As mentioned above, the zone to be considered is located in the supercritical domain just above the critical point; it is not meaningful to consider it for higher pressures and temperatures. As previously reminded, the end point of the Widom line of pure carbon dioxide is roughly around 314 K and 88.6 bar. This pseudo-boiling zone must be avoided in order to limit the fluid property variations for small variations of pressure and temperature. Since there are thermal gradients in high-pressure vessels, due to heat transfer limitations or poor insulation, as well as inevitable pressure

gradients due to the fluid flow and the resulting pressure losses, it would be recommended to choose a working pressure well outside the pseudo-boiling zone.

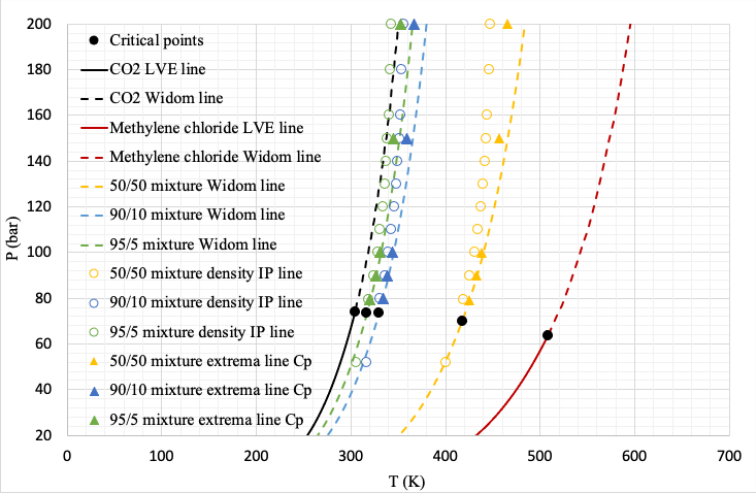

Figure 7: Widom lines, extrema lines and inflexion point lines predicted for the CO_2/Methylene chloride binary mixtures.

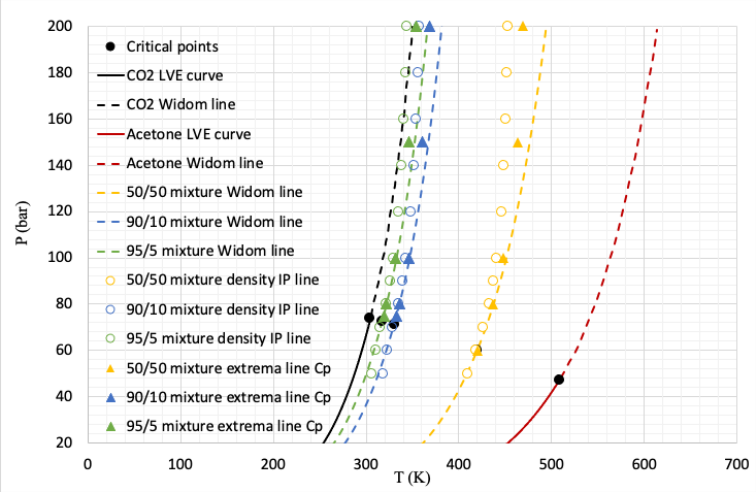

Figure 8: Widom lines, extrema lines and inflexion point lines predicted for the CO_2/acetone binary mixtures.

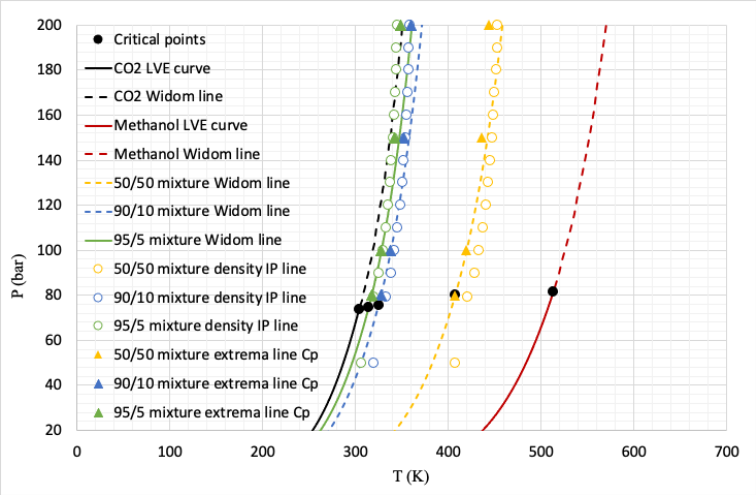

Figure 9: Widom lines, extrema lines and inflexion point lines predicted for the CO_2/methanol binary mixtures.

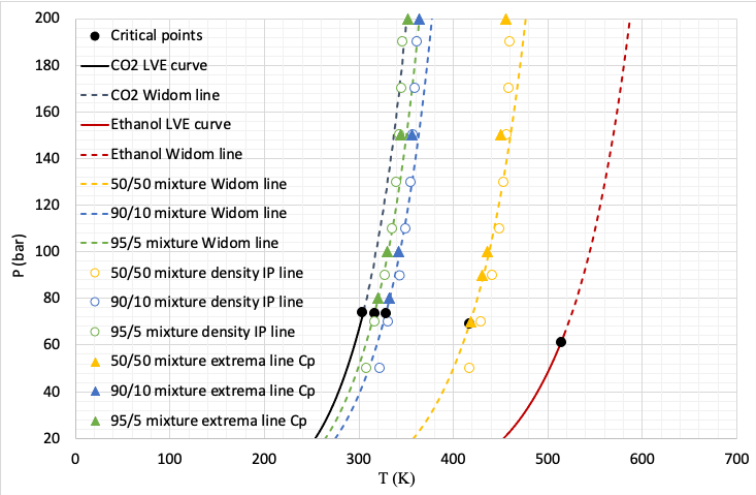

Figure 10: Widom lines, extrema lines and inflexion point lines predicted for the CO_2/ethanol binary mixtures.

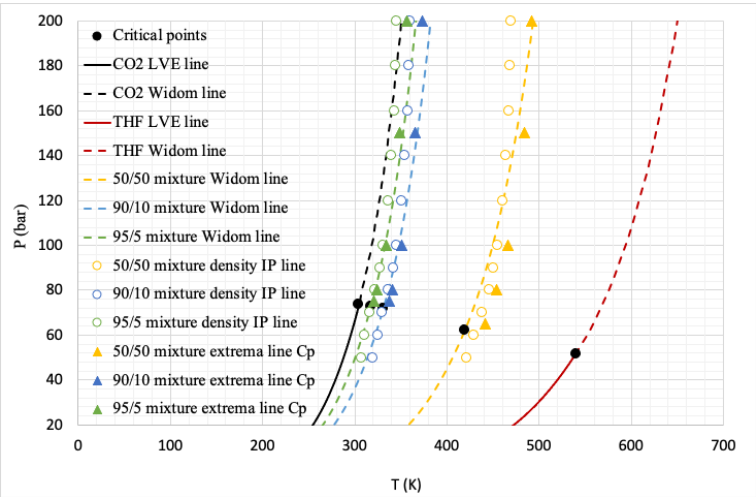

Figure 11: Widom lines, extrema lines and inflexion point lines predicted for the CO_2/THF binary mixtures.

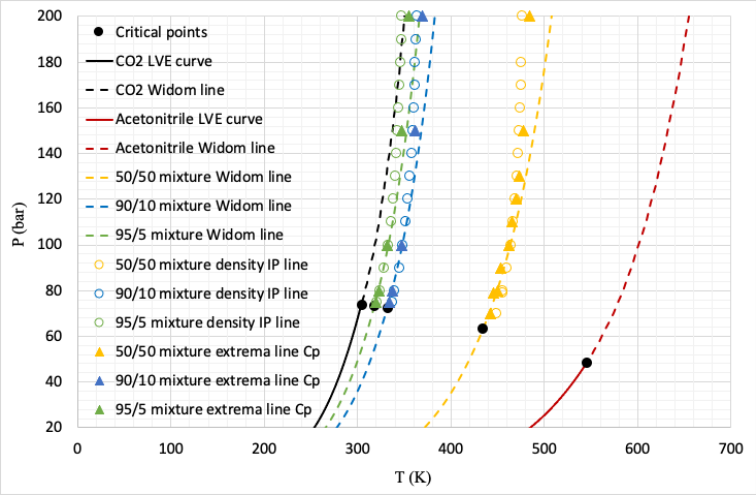

Figure 12: Widom lines, extrema lines and inflexion point lines predicted for the CO_2/acetonitrile binary mixtures.

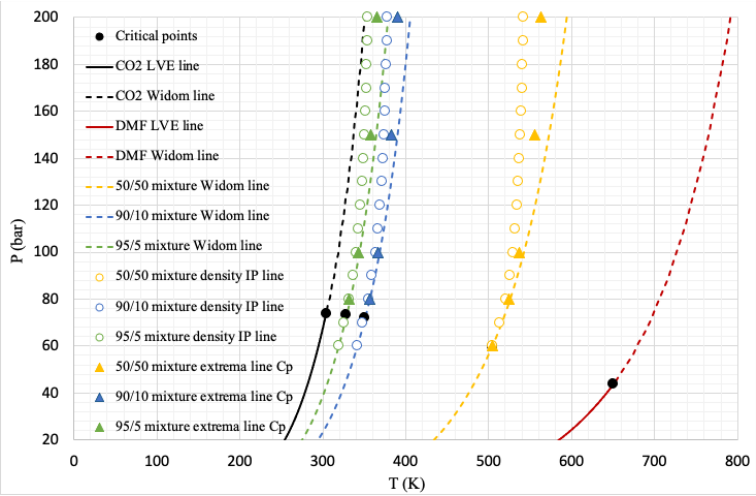

Figure 13: Widom lines, extrema lines and inflexion point lines predicted for the CO_2/DMF binary mixtures.

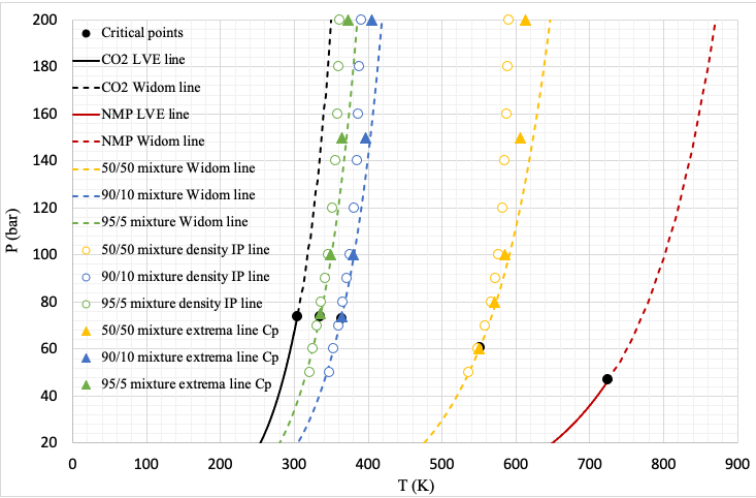

Figure 14: Widom lines, extrema lines and inflexion point lines predicted for the CO_2/NMP binary mixtures.

3.2.2. Type III phase behavior mixtures

The predicted Widom lines, extrema lines and inflexion point lines for pure compounds and for binary mixtures involving CO_2 with water are presented in Figure 15. The Widom line of pure CO_2, of pure water as well as those of the binary mixtures (5, 10 and 50 % of water) are plotted. The mixture extrema lines and the density inflexion point lines are also plotted. For the sake of clarity, we did not plot the results for other CO_2/water mixture compositions. Nevertheless, all the details are given in the previous section for the calculation of any composition of water in the mixture.

There are many applications for which supercritical CO_2 is used in mixture with water, sometimes saturated with water. These results can help in choosing the operating conditions in the supercritical region while avoiding the transition zone, located just above the critical point. As reminded above, the end point of the Widom line of pure water is roughly around 683 K and 311 bar, while that of carbon dioxide is around 314 K and 88.6 bar.

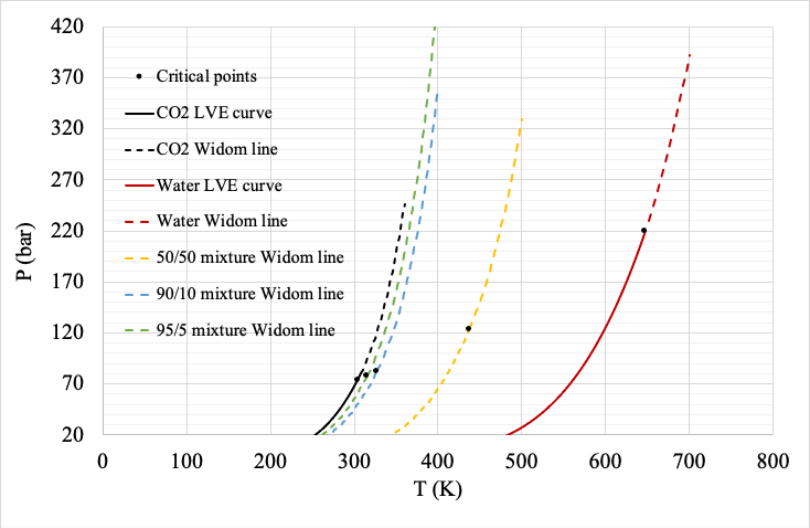

Figure 15: Widom lines, extrema lines and inflexion point lines predicted for CO_2/water binary mixtures.

3.3. Transitory zones and supercritical process conditions

As already discussed above, the Widom line, extrema lines and inflexion point lines correspond to transitory zones where fluid properties undergo dramatic fluctuations for small variations in pressure and temperature. As the critical point is avoided, operating conditions corresponding to these transitory zones must be avoided. Even if it concerns a rather small domain of pressure and temperature (area just above the critical point), it can concern several applications of supercritical fluid technology such as cleaning, purification, fractionation, particle generation, functionalization/impregnation, sterilization and in a less extent extraction, since for this latter process, pressures higher than 100 bar are always used.

For every application of supercritical carbon dioxide, a compromise must be found between the process efficiency and the economic aspects. It is therefore preferable to work at low pressures and temperatures which corresponds to approaching the transitory zones. For applications involving a solute solubilization step in carbon dioxide, as is the case among others, of extraction, fractionation or impregnation, the operating conditions are generally chosen by considering the retrograde solubility of the solute. The retrograde solubility zone, covering the critical point, corresponds to a domain for which an increase in temperature leads to a decrease in solubility. From a certain value of pressure, this is no longer observed and an increase in temperature leads to an increase in solubility. This means that for lower pressures, the retrograde solubility behavior is observed, and the lowest temperatures are then favored. Ordinarily, this domain corresponds or is close to the pseudo-boiling zone. In this case, it is therefore advisable to consider the Widom lines and the extrema lines so as to choose the right operating conditions, hence avoiding property fluctuations that can lead to poor reproducibility and thus poor process control.

4. Conclusion

In this work, it has been demonstrated that the Widom lines, extrema lines and inflexion point lines of binary mixtures involving CO_2 can be predicted and that it is meaningful to consider them in order to choose the best process operating conditions. More specifically, the conditions of the pressure and temperature of supercritical processes must be chosen outside these transitory zones. The choice of the best operating conditions depends on the targeted application. If the main goal is to have high SCF solvent power (extraction, fractionation, …), the operating conditions must correspond to the zone above the Widom line, in which the SCF behaves like a liquid, with a high density. If the main SCF property required is high diffusivity (reactions), the operating zone will more likely be below the Widom line. The different approaches proposed for the prediction of the location of the transitory zones in a PT diagram can be applied to binary mixtures involving CO_2 for any composition.

References

[1] G. Brunner, Supercritical Fluids as Solvents and Reaction Media, Elsevier Science, 2004. https://doi.org/10.1016/B978-0-444-51574-2.X5000-7

[2] R. Smith, H. Inomata, C. Peters, Introduction to supercritical fluids: A spreadsheet-based Approach, Elsevier, 2013.

[3] A.R. Duarte, Current trends of Supercritical Fluid Technology in Pharmaceutical, Nutraceutical and Food Processing Industries, Bentham Books, 2018. https://doi.org/10.2174/97816080504681100101

[4] M. Perrut, V. Perrut, Supercritical Fluid applications in the Food Industry, Gases in Agro-Food processes (2019) 483-509. https://doi.org/10.1016/B978-0-12-812465-9.00020-7

[5] G. Soares, D. Learmonth, M. Vallejo, S. Perez Davilla, P. Gonzalez, R. Sousa, A. Oliveira, Supercritical CO2 technology: The next standard sterilization technique?, Materials science and engineering: C 99 (2019) 520-540, https://doi.org/10.1016/j.msec.2019.01.121

[6] M.E. Fisher, B. Widom, Decay of correlations in linear systems, J. Chem. Phys. 50 (1969) 3756–3772. https://doi.org/10.1063/1.1671624

[7] D.T. Banuti, Crossing the Widom-line – Supercritical pseudo-boiling, J. of Supercritical Fluids 98 (2015) 12–16. https://doi.org/10.1016/j.supflu.2014.12.019

[8] M. Oschwald, A. Schik, Supercritical nitrogen free jet investigated by spontaneous Raman scattering, Experiments in Fluids 27 (1999) 497–506. https://doi.org/10.1007/S003480050374

[9] M. Oschwald, M. Micci, Spreading angle and centerline variation of density of supercritical nitrogen jets, Atomization and Sprays 11 (2002) 91–106. https://doi.org/10.1615/AtomizSpr.v12.i123.50

[10] M. Santoro, F. Gorelli, 2008. Structural changes in supercritical fluids at high pressures, Physical Review B. 77, 212103. https://doi.org/10.1103/PhysRevB.77.212103

[11] T. Sato, M. Sugiyama, K. Itoh, K. Mori, T. Fukunaga, M. Misawa, T. Otomo, S. Takata, 2008. Structural difference between liquidlike and gaslike phases in supercritical fluid, Phys. Rev. E. 78, 051503. https://doi.org/10.1103/PhysRevE.78.051503

[12] M. Raju, D.T. Banuti, P.C. Ma, M. Ihme, 2017. Widom Lines in Binary Mixtures of Supercritical Fluids, Sci. Rep. 7, 3027. https://doi.org/10.1038/s41598017-03334-3

[13] E.N. de Jesús, J. Torres-Arenas and A.L. Benavides, 2021. Widom line of real substances, J. Mol. Liq. 322, 114529. https://doi.org/10.1016/ j.molliq.2020.114529

[14] I. M. Zerón, J. Torres-Arenas, E. N. de Jesús, B. Ramírez, and A. L. Benavides, 2019. Discrete potential fluids in the supercritical region, J. Mol. Liq. 293, 111518. https://doi.org/10.1016/j.molliq.2019.111518

[15] I.H. Bell, G. Galliero, S. Delage-Santacreu, L. Costigliola, 2020. An entropy scaling demarcation of gas- and liquid-like behaviors, J. Chem. Phys. 152, 191102. https://doi.org/10.1063/1.5143854

[16] R.H. Van Konynenburg, R.L. Scott, Critical lines and phase equilibria in binary van der waals mixtures, Philos. Trans. R. Soc. Lond. Ser. A Math. Phys. Sci. 298 (1980) 495-540. https://doi-org/10.1098/rsta.1980.0266

[17] M. Stievano, N. Elvassore, High-pressure density and vapor–liquid equilibrium for the binary systems carbon dioxide–ethanol, carbon dioxide–acetone and carbon dioxide–dichloromethane, J. of Supercritical Fluids 33 (2005) 7–14. https://doi.org/10.1016/j.supflu.2004.04.003

[18] M.J. Lazzaroni, D. Bush, J.S. Brown, C.A. Eckert, High-Pressure Vapor-Liquid Equilibria of Some Carbon Dioxide + Organic Binary Systems, J. Chem. Eng. Data 2005, 50, 60-65. https://doi.org/10.1021/je0498560

[19] Ch.J. Chang, Ch.-Y. Chen, H.-Ch. Lin, J. Chem. Eng. Data 40 (1995) 850–855. https://doi.org/10.1021/je00020a025

[20] M.F. Monteiro, M.H. Moura-Neto, C.G. Pereira, 2020. Description of phase equilibrium and volumetric properties for CO_2+water and CO_2+ethanol using the CPA equation of state. J. of Supercritical Fluids 161, 104841. https://doi.org/10.1016/j.supflu.2020.104841

[21] J.M. Miguez, M. Pineiro, J. Algaba, B. Mendiboure, J.P. Torré, F.B. Jimenez, Understanding the Phase Behavior of Tetrahydrofuran + Carbon Dioxide, + Methane, and + Water Binary Mixtures from the SAFT-VR Approach, J. Phys. Chem. B 119 (2015) 14288-14302. https://doi.org/10.1021/acs.jpcb.5b07845

[22] A. Aasen, M. Hammer, G. Skaugen, J.P. Jacobsen, O. Wilhelmsen, Thermodynamic models to accurately describe the PVTxy-behavior of water/carbon dioxide mixtures, Fluid Phase Equilib. 442 (2017) 125-139. https://doi.org/10.1016/j.fluid.2017.02.006

[23] R.H. Perry, D.W. Green, J.O. Maloney, eds., Perry's chemical engineers' handbook, 7th ed, McGraw-Hill, New York, 1997.

[24] P. Linstrom, NIST Chemistry WebBook, NIST Standard Reference Database 69, (1997). https://doi.org/10.18434/T4D303

[25] R.C. Reid, J.M. Prausnitz, B.E. Poling, The properties of gases and liquids, 4th ed, McGraw-Hill, New York, 1987.

[26] D.T. Banuti, M. Raju, M. Ihme, 2017. Similarity law for Widom lines and coexistence lines. Phys. Rev. E. 95, 052120. https://doi.org/10.1103/PhysRevE.95.052120

[27] G. Guevara-Carrion, S. Ancherbak, A. Mialdun, J. Vrabec, V. Shevtsova, 2019. Diffusion of methane in supercritical carbon dioxide across the Widom line. Sci. Rep. 9, 8466.

Supplementary materials

Table 2: The calculated critical properties and acentric factors of the binary mixtures CO_2/solvent

CO_2 /	x_1	T_{cm} (K)	P_{cm} (bar)	V_{cm} ($m^3 \cdot mol^{-1}$)	ω
Methanol	0.50	407.4	80.07	$1.05.10^{-5}$	0.395
	0.90	324.6	75.52	$9.61.10^{-5}$	0.2581
	0.95	314.4	74.7	$9.50.10^{-5}$	0.241
Ethanol	0.50	417.4	69.14	$12.92.10^{-5}$	0.4335
	0.90	328.5	73.45	$10.07.10^{-5}$	0.2658
	0.95	316.5	73.69	$9.73.10^{-5}$	0.2449
1-methyl-2-pyrrolidone (NMP)	0.50	550.9	60.71	$19.15.10^{-5}$	0.2955
	0.90	363.7	73.08	$11.17.10^{-5}$	0.2382
	0.95	334.9	73.74	$10.27.10^{-5}$	0.2311
Tetrahydrofuran (THF)	0.50	419.3	62.25	$15.47.10^{-5}$	0.231
	0.90	330.9	71.72	$10.53.10^{-5}$	0.2253
	0.95	317.8	72.81	$9.96.10^{-5}$	0.2246
Acetone	0.50	419.6	60	$14.87.10^{-5}$	0.2655
	0.90	330.4	71.37	$10.51.10^{-5}$	0.2323
	0.95	317.5	72.68	$10.00.10^{-5}$	0.2281
Water	0.50	437.9	123.4	$7.41.10^{-5}$	0.2835
	0.90	326.8	81.54	$8.98.10^{-5}$	0.2358
	0.95	315.3	77.57	$9.19.10^{-5}$	0.2299
Acetonitrile	0.50	434.1	63.2	$13.21.10^{-5}$	0.282
	0.90	332	72.53	$10.21.10^{-5}$	0.2356
	0.95	318.2	73.29	$9.85.10^{-5}$	0.2298
N,N-Dimethyl Formamide (DMF)	0.50	503.9	59.57	$17.09.10^{-5}$	0.268

	0.90	350.8	72.23	$10.82.10^{-5}$	0.2327
	0.95	328.1	73.21	$10.10.10^{-5}$	0.2283
	0.50	417.7	69.76	$14.05.10^{-5}$	0.232
Methylene chloride	0.90	329.5	73.5	$10.27.10^{-5}$	0.2255
	0.95	317	73.71	$9.83.10^{-5}$	0.2247